Pure Appl. Chem., Vol. 76, Nos. 7–8, pp. 1421–1433, 2004.

Organic electro-optic materials*

Larry R. Dalton

Department of Chemistry, University of Washington, Seattle, WA 98195-1700, USA

Abstract: The macroscopic electro-optic activity of organic materials depends upon the molecular hyperpolarizability, β, of individual organic chromophores and upon the product of number density, *N*, and noncentrosymmetric order, $\langle\cos^3\theta\rangle$, of the chromophores in a hardened polymer lattice. Quantum and statistical mechanical calculations provide the basis for rational improvement of these parameters leading to electro-optic coefficients (at telecommunication wavelengths) of greater than 100 pm/V (a factor of 3 larger than values for the best inorganic material, lithium niobate). Such calculations also provide insight into what further improvements can be expected. Owing to low and relatively dispersionless dielectric constants and refractive indicies, organic materials facilitate the fabrication of devices with 3 dB operational bandwidths of greater than 100 GHz. Moreover, robust and low optical loss materials can be fabricated by design. An under-appreciated advantage of organic electro-optic materials is their processability, and a variety of stripline, cascaded prism and superprism, and ring microresonator devices are readily fabricated. Conformal, flexible, and three-dimensional devices are also readily produced. With ring microresonator devices, active wavelength division multiplexing, optical network reconfiguration, and laser frequency tuning are straightforwardly accomplished.

INTRODUCTION

The potential of organic materials for fabrication of high bandwidth, low drive voltage electro-optic devices has long been appreciated [1–7]. The bandwidth potential is defined by the fundamental response time of the π-electron systems of unsaturated organic materials, namely, the phase relaxation of the π-electrons. Phase relaxation times for π-electron organics lie in the femtosecond time regime, and, thus, bandwidths of hundreds of gigahertz or even tens of terahertz are, at least, possible. In practice, operation of organic electro-optic devices requires the simultaneous propagation of both electrical and optical signals through the material. The electrical signals must typically be brought to the material through metal wires (electrodes) and connectors, and these components limit device bandwidths, e.g., to 3-dB bandwidths on the order of 200 GHz [8,9].

Quantum mechanics have long been used to guide the improvement of the molecular first hyperpolarizability, β, of organic chromophores [10–13]. While such calculations do not usually quantitatively reproduce experimental molecular β values, they are useful in reproducing qualitative trends for the change of β with chromophore structure variation. In the next section, we will demonstrate how even minor structural modifications of charge transfer (π-electron donor—π-electron bridge—π-electron acceptor) chromophores can lead to significant improvement in β.

A more serious problem impeding the development and employment of organic electro-optic materials relates to the difficulty of achieving a noncentrosymmetric (dipolar or ferroelectric) lattice of densely packed chromophores. This is because dipole–dipole interactions among chromophores favor

*Lecture presented at the symposium "Polymers in electronics and photonics: Synthesis, characterizations and device applications", as part of the 39th IUPAC Congress and 86th Conference of the Canadian Society for Chemistry: Chemistry at the Interfaces, Ottawa, Canada, 10–15 August 2003. Other Congress presentations are published in this issue, pp. 1295–1603.

centrosymmetric (anti-ferroelectric) arrangement of chromophores. Actually, this is somewhat of an oversimplification in that dipole–dipole interactions are spatially anisotropic and the approach along their poles actually favors noncentrosymmetric (ferroelectric) ordering of the dipolar chromophores. That is, there are competing ferroelectric and anti-ferroelectric ordering potentials associated with dipole–dipole interactions, and the relative importance of these contributions to overall order can be tuned by control of chromophore shape. The magnitude of the problem of translating molecular first hyperpolarizability into macroscopic electro-optic activity can be appreciated when it is realized that chromophore loading of 30 % and an order parameter of 0.3 is considered outstanding. Such values mean that only 9 % of the molecular hyperpolarizability of a chromophore is being translated to macroscopic electro-optic activity. In practice, translation efficiencies of only a few percent are more common. The exceptional optimism expressed in the 1980s and early 1990s concerning electro-optic activity that could be achieved with organic electro-optic materials failed to appreciate the difficulty of translating molecular hyperpolarizability into macroscopic electro-optic activity. Indeed, independent particle theoretical analyses were typically employed to estimate macroscopic electro-optic coefficients (r_{33} and r_{13}) for electrically poled polymers during this period. The Figure of Merit for an electro-optic chromophore was considered to be the product of dipole moment and molecular first hyperpolarizability divided by molecular weight. In reality, electro-optic activity for high-dipole-moment chromophores is routinely observed to exhibit a maximum as a function of chromophore number density, thus invalidating the above Figure of Merit. Correct treatment of intermolecular interactions among many particles is not a trivial problem, but is absolutely necessary because of the large (e.g., 10–20 D) dipole moments associated with high molecular hyperpolarizability charge-transfer chromophores. Dalton and Robinson [7,13–20] have tackled this problem using both analytical and numerical (computer simulation) approaches.

Analytical derivations involve defining an intermolecular potential function describing the electrical fields that a reference chromophore feels from a large ensemble of surrounding chromophores as well as the potential function describing the interaction of the reference chromophore with an applied electric poling field. Such intermolecular interactions include both electronic (from chromophores and polymer host) and nuclear (steric) interactions. We have shown that the simple independent particle order parameter, $<\cos^3\theta> = \mu F/5kT$ where μ is the chromophore dipole moment, F is the electric poling field felt by the reference chromophore, k is the Boltzmann constant, and T is the Kelvin temperature, must be modified to include a Langevin attenuation factor that depends upon chromophore number density, N, or in other words upon chromophore loading. Analytical theory is quite successful in reproducing the behavior observed for electro-optic activity vs. chromophore number density (loading) for chromophores physically incorporated into polymers such as amorphous polymer carbonate (APC [7]) and polymethylmethacrylate (PMMA) to form composites. Analytical theory correctly predicts that a maximum is observed in the graph of electro-optic activity vs. chromophore number density and that the position of that maximum is approximately given by $N_{max} = 1.38T/\mu^2$ (neglecting steric or chromophore shape effects). The most important observation to derive from analytical theory is that electronic and nuclear (steric or chromophore shape) interactions can be designed to have different spatial anisotropies as the former will depend only upon the π-electron distribution, while the latter will depend on all atoms comprising the chromophore. The worst possible shape for an electro-optic chromophore is that of a prolate ellipsoid. Making chromophores more spherical shifts N_{max} to larger values and increases the maximum obtainable electro-optic activity [19,20]. Indeed, this observation permitted design and preparation of the first organic electro-optic materials to exhibit an electro-optic coefficient exceeding that of lithium niobate at telecommunication wavelengths (1.3 and 1.55 μm). These materials were also the first to permit Mach Zehnder devices to be fabricated that exhibited operational voltages of less than 1 volt at telecommunication wavelengths [21,22].

Covalent incorporation of electro-optic chromophores into polymeric (or macromolecular) matrices creates a situation that is more difficult to theoretically analyze, and indeed we have resorted to numerical methods to treat this problem [7,13,16,18–20]. With covalent attachment, chromophores can no

longer be assumed to move independently of the host lattice even near the glass transition temperature (where electric field poling is carried out to introduce noncentrosymmetric order that is subsequently locked in place by chemical crosslinking and by cooling the sample). An effective approach to considering the additional potential interactions associated with covalent coupling appears to be the pseudo-atomistic Monte Carlo method [19,20] where the stiff π-electron chromophores are treated as rigid objects (analogous to the United Atom Approach), while the remaining flexible components of the material are treated atomistically [19,20,23]. The pseudo-atomistic Monte Carlo method permits the restrictions on motion associated with covalent bonds to be accounted for appropriately in the numerical simulation of chromophore order. Monte Carlo methods have the added advantage of providing snap shot pictures of minimum-energy chromophore distributions associated with various trajectories. In the following section, we demonstrate how theory can be used to gain at least qualitative insight into chromophore order for chromophores incorporated into dendrimer and dendronized polymers.

While electro-optic activity and frequency response (bandwidth) attract the most attention from those contemplating the use of organic electro-optic materials for the fabrication of devices, other properties must also be considered. Optical loss is important, and three components of loss must be considered: (1) material absorption loss, (2) material scattering loss, and (3) device insertion loss [i.e., loss associated with impedance matching of passive and active (electro-optic) waveguide structures]. Absorption loss, at telecommunication wavelengths, is dominated by overtone absorptions associated with hydrogen; thus, reduction of material loss to desired values of 1 dB/cm or less requires minimizing hydrogen density including by means such as fluorination. Material loss values as low as 0.1–0.2 dB/cm have been obtained with heavily fluorinated chromophore-containing dendrimer materials [13]. Scattering loss can typically be associated with some aspect of material processing and involves either material heterogeneity (arising in processes such as spin casting, electric field poling, or lattice hardening subsequent to poling [15,24]) or material damage (arising during electric field poling, deposition of cladding layers, or waveguide fabrication by reactive ion etching or photolithographic methods). The discussion of scattering loss mechanisms is a topic requiring more space than available in this communication, and the reader is referred elsewhere for more insight into this topic [6,7,15,24]. However, it should be noted that, with care, scattering loss can be kept to very low values and electro-optic waveguide loss of 1 dB/cm or less can be obtained with attention to the details of processing. Insertion loss is defined by the combination of absorption, scattering, and optical mode impedance matching losses. With organic electro-optic waveguides mode size mismatch is the greatest source of loss in going from passive (typically silica) to active (organic electro-optic) waveguide. This is because low loss silica waveguides are spherical with active core diameters on the order of 10 μm while organic electro-optic waveguides are typically ellipsoidal with cross-sectional dimensions on the order of 2×6 μm. The mode size mismatch problem is typically solved by use of some type of mode transformation structure [25,26]. These structures can be readily realized by reactive ion etching using special mask structures and optical loss values as low as 0.2 dB per transition have been obtained (the exact values depend on the length of the transition structure). When great care is exercised, total insertion loss on the order of 3 dB can be obtained for a 2-cm organic electro-optic modulator device although total insertion loss values of 5–10 dB are more common. It must be noted that cladding materials can contribute to optical loss through optical fields fringing into these materials and through interfacial problems between core and cladding materials. In summary, although optical loss is an important problem demanding detailed attention through all stages of material development and processing, contributions to final total insertion loss appear to be well understood and controllable within acceptable limits.

Organic electro-optic materials must be stable including under conditions of elevated temperature, high optical power, and space radiation. Thermal stability is typically associated with thermally induced loss of electric-field-poling-induced noncentrosymmetric order [27–29]. For composite materials, temperature stability can be associated with the glass transition of the final polymer matrix, i.e., poling induced order is lost at an increasingly rapid rate as the difference between device operating temperatures and the glass transition temperature of the organic electro-optic material is decreased.

Improved thermal stability has traditionally been achieved by lattice hardening, i.e., chemical crosslinking subsequent to electric field poling [27–29]. Chemical functionalities are added to chromophores that permit chemical cross linking of the chromophores to a three-dimensional supermolecular matrix while the electric poling field is on. Two classes of crosslinking reactions have been investigated: (1) Thermally induced crosslinking and (2) photoinduced crosslinking [27–29]. With thermally induced crosslinking reactions, the temperature dependence of the crosslinking reaction must be compatible with temperatures used in electric field poling. Otherwise, considerable reduction in poling efficiency results. Thermally induced crosslinking chemistries utilized in the 1990s frequently involved condensation reactions and the elimination of water. Such crosslinking can be sensitive to atmospheric moisture and it is difficult to maintain the desired reaction stoichiometry [24]. More recently, cross linking reactions that avoid this problem have been introduced [30]. With thermally induced crosslinking, poling and crosslinking are typically effected using a "stepped" protocol whereby temperature and electric poling field strength are increased in a stepped manner with time. With photoinduced crosslinking reaction, care must be exercised to avoid competitive absorption of light by the electro-optic chromophore and the photo-initiator. The obvious advantage of photocrosslinking is that it can be de-coupled from the temperature-dependent poling process. To the present time, photo-crosslinking has not proven to be a viable route to lattice hardening of organic electro-optic materials although this is likely to change in the future based on recent (unpublished) results in our laboratory.

Organic electro-optic materials appear to be stable to space radiation (gamma rays and high-energy particles). The π-electron system of these materials may act to help dissipate electronic perturbation associated with space radiation/particle bombardment. Photochemical stability, particularly in the presence of oxygen, appears to be a more serious problem [13]. Singlet oxygen chemistry appears to define the dominant photochemical degradation pathways although an intramolecular condensation reaction pathway has been identified for substituted stilbenes leading to phenanthrenes [31]. Several things can be done to improve stability, including lattice hardening (which slows down the diffusion of singlet oxygen and reactive species), the use of physical and chemical singlet oxygen quenchers, and exclusion of oxygen by packaging [13,32]. Photochemical stability can also be significantly improved by eliminating or sterically protecting chromophore sites subject to singlet oxygen attack. With attention to detail, it appears that materials appropriate for applications involving telecommunication optical power levels can be produced [13,32].

Both electronic and ionic conductivity must be controlled in organic materials to avoid attenuation of electric fields during poling and bias voltage drift during operation of electro-optic modulators. One wants to design chromophores for maximum hyperpolarizability (charge displacement under an applied electric field), but one must contain the perturbation within the chromophore. Polymers with extended π-electron segments, such as poly(*p*-phenylene), are in general not appropriate hosts for electro-optic chromophores because charge can be transferred to these host materials, leading to phenomena such as photoconductivity. Fortunately, rational control of supramolecular chromophore order necessary to maximize electro-optic activity can also be used to control electrical conductivity. Ionic conductivity can be controlled by careful purification of materials.

The fabrication of waveguide devices from organic electro-optic materials requires control of index of refraction, dielectric, optical loss, and electrical conductivity properties of both core (electro-optic) and cladding waveguide materials. To this point in time, very little consideration has been given to cladding materials. This is a situation that will have to change as organic electro-optic materials move forward toward broader commercial application.

A distinct advantage of organic electro-optic materials is their processability. Conformal and flexible devices are readily fabricated and three-dimensional device structures can be fabricated. A wide range of stripline, cascaded prism and superprism, and ring microresonator structures have been fabricated and evaluated for applications ranging from phased array radar, to optical gyroscopes, to spatial light modulation, to active wavelength division multiplexing.

Obviously, it is beyond the scope of this communication to treat all aspects of recent progress in the area of organic electro-optic materials. In the following sections, we attempt to provide a brief discussion of recent progress in the areas of (1) chromophore design, (2) optimization of translation of molecular hyperpolarizability to macroscopic electro-optic activity, and (3) advances in the fabrication of ring microresonators.

IMPROVEMENT OF CHROMOPHORES

The use of semi-empirical quantum mechanical and density functional theory (DFT) methods [13,33] to improve chromophore hyperpolarizability is illustrated in Fig. 1. In this figure, we show the theoretically predicted variation of molecular hyperpolarizability, β, dipole moment, μ, and the maximum of the interband (HOMO-LUMO) charge-transfer absorption, λ_{max}, with changing structure of the acceptor group of the chromophore. For the structures shown, good agreement exists between DFT and semi-empirical results. The structures in the upper left- and right-hand sides of the figure differ by replacement of a single methyl group on the tricyanofuranvinylene (TCF) acceptor with a trifluoromethyl group. This particular structural modification has been investigated by researchers at Lockheed Martin [34] and Corning [35,36] as well as by our research group, with the observation that $–CF_3$ replacement of a $–CH_3$ group consistently leads to improved β in reasonable quantitative agreement with the predictions of theory.

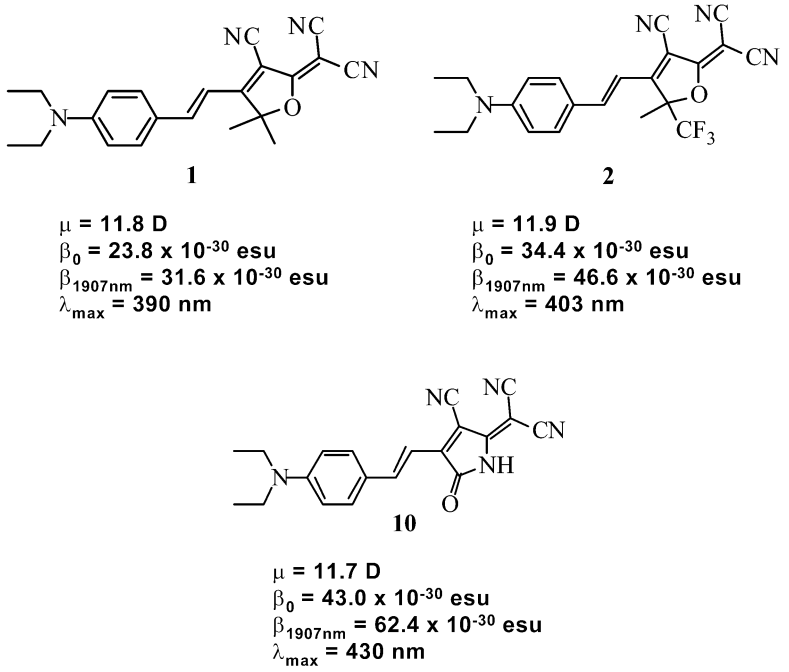

Fig. 1 Calculated values for dipole moment, μ, molecular hyperpolarizability in the long wavelength limit, β_0, molecular hyperpolarizability at 1907 nm, and the wavelength of the maximum of the interband charge transfer absorption are shown for several modification of the acceptor functionality of a donor–bridge–acceptor charge-transfer chromophore.

Replacement of the TCF acceptor with a tricyanopyrrolinevinylene (TCP) acceptor is predicted to lead to even greater improvement in molecular hyperpolarizability and ultimately electro-optic activity (see Scheme 1 for one synthetic pathway to the TCP model compound). This has been observed to be true not only for model compounds (characterized by hyper-Rayleigh scattering, HRS, measure-

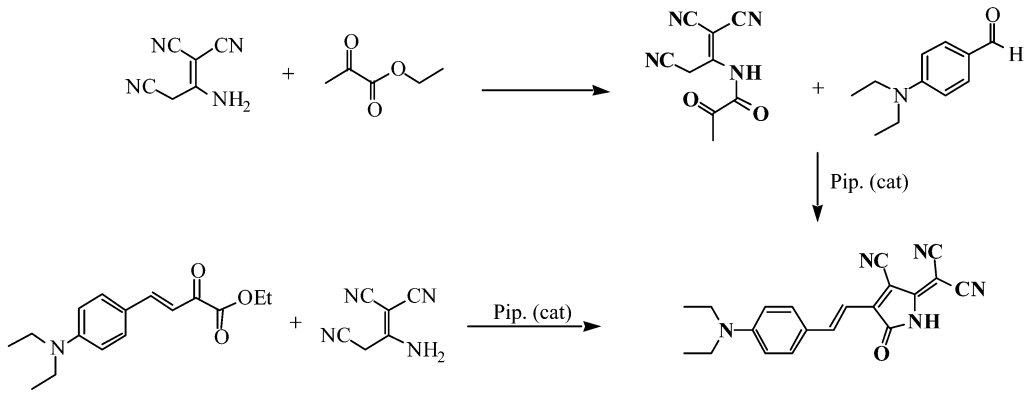

Scheme 1 A synthesis of the TCP model compound is shown. See also ref. [37] for a discussion of microwave-assisted synthesis (particularly of TCF and TCP acceptors).

ments of β), but for the chromophore of Fig. 2. Note that an electro-optic activity of 101 pm/V is obtained for the chromophore of Fig. 2 for only 20 % loading (by weight) in amorphous polycarbonate. This is an exceptional result for such a relatively short chromophore. An additional advantage of the TCP acceptor is that it is amenable to derivatization, which can facilitate attachment of both ends of the chromophore to a host lattice. This acceptor also affords some advantages with respect to ease of synthesis and stability.

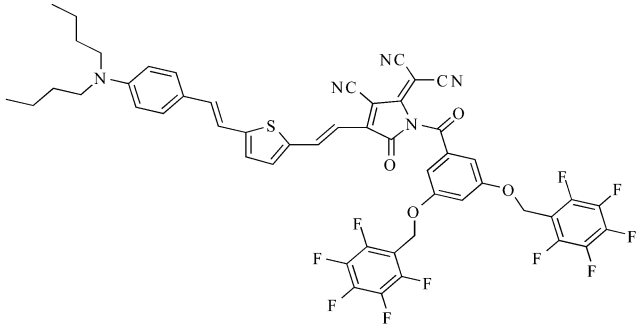

Fig. 2 An electro-optic chromophore based on the tricyanopyrrolinevinylene (TCP) acceptor yields and electro-optic coefficient of 101 pm/V at 1.55 μm when incorporated into amorphous polycarbonate (20 wt %).

Of course, many other modifications of chromophore structures, involving the donor, bridge, and acceptor portions of the chromophore, are predicted to lead to further improvement. For example, a "gradient bridge"-type chromophore where a weak donor (e.g., thiophene) is located near the strong amine donor and a weak acceptor (thiazole) is located near the strong acceptor (TCF or TCP) is predicted to lead to improvement in molecular first hyperpolarizability relative to a "homogeneous" bridge structure (e.g., two thiophene groups). An example of a gradient bridge structure is shown in Fig. 3. Again, while quantum mechanical calculations do not yield quantitative reproduction of experimental data, they do appear to provide very useful qualitative insight for predicting the effect of simple chromophore modifications.

The important conclusion to be drawn from the above observations is that there will likely be continuing improvements in molecular hyperpolarizability for some time to come. This trend alone will likely result in electro-optic coefficients of organic materials exceeding 200 pm/V over the next several years. (Indeed, a material exhibiting an electro-optic coefficient of 182 pm/V at 1.3 μm has recently

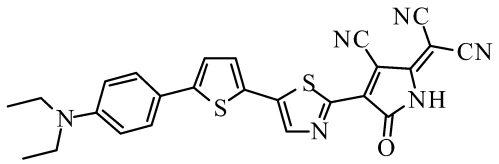

150

μ = 13.5 D
β_0 = 188.0 x 10^{-30} esu
β_{1907nm} = 399.3 x 10^{-30} esu
λ_{max} = 600 nm

Fig. 3 Calculated values for dipole moment, μ, molecular hyperpolarizability in the long wavelength limit, β_0, molecular hyperpolarizability at 1907 nm, and the wavelength of the maximum of the interband charge transfer absorption are shown for "gradient bridge"-type chromophore.

been prepared in our laboratory based on the principles discussed in this communication. This value will need to be independently verified, but speaks to the likely validity of the speculation just made.) Even greater values of electro-optic activity could be achieved with an improvement in the efficiency of translating molecular hyperpolarizability into macroscopic electro-optic activity can be achieved.

An important issue in developing new electro-optic chromophores is synthetic efficiency. Obviously, a detailed discussion of this topic is beyond the scope of this communication; however, we point out that microwave-assisted synthesis [37] has proven particularly useful for reducing reaction times and improving yields for a number of reactions common to the production of charge transfer-type organic electro-optic chromophores. The reader is also referred to refs. [7,38–40] for an introduction to and specific discussion of the fundamental types of reaction pathways to organic electro-optic materials, including the most commonly used pathway based on the Knoevenagel coupling of aldehydes.

IMPROVED TRANSLATION OF MOLECULAR HYPERPOLARIZABILITY TO MACROSCOPIC ELECTRO-OPTIC ACTIVITY

We have already noted that either analytical or Monte Carlo theoretical methods can be used to understand the variation of electro-optic activity with chromophore number density in chromophore/polymer composite materials. To understand electro-optic activity observed for chromophores covalently incorporated into multi-chromophore dendrimers and dendronized polymers, one must resort to atomistic or pseudo-atomistic Monte Carlo calculations [19,20,23]. Because of the size of the macromolecular and supramolecular structures considered in our research, we focus on pseudo-atomistic Monte Carlo methods [20,23] where rigid segments are treated as rigid objects (analogous to the United Atom approach) and flexible segments of the macromolecular structure are treated atomistically. Note that a wide range of potential functions ranging from those associated with free rotation about single bonds to potential functions derived from high-level quantum mechanical calculations can be and are employed. In Fig. 4, we illustrate an attempt to understand large electro-optic activity observed in the three-chromophore dendrimer experimental studies of Jen and coworkers [41].

The large electro-optic activity observed by Jen and coworkers [41] appears to derive from the three chromophores assuming a "J-aggregate-like" spatial arrangement, where two of the chromophores are positioned head-to-tail and the third chromophore is at the "magic angle" with respect to the other two. The calculated structure shown in Fig. 4 is the structure expected in the limit of very high poling fields. In practice, such fields are not usable because they exceed dielectric breakdown of the electro-optic material. For experimental poling field strengths, the simulated structure is somewhat more disordered. However, pseudo-atomistic Monte Carlo calculations are clearly useful in understanding the conformations that can be assumed in multi-chromophore dendrimers and how these conformations account for the large electro-optic activity observed for certain dendritic materials.

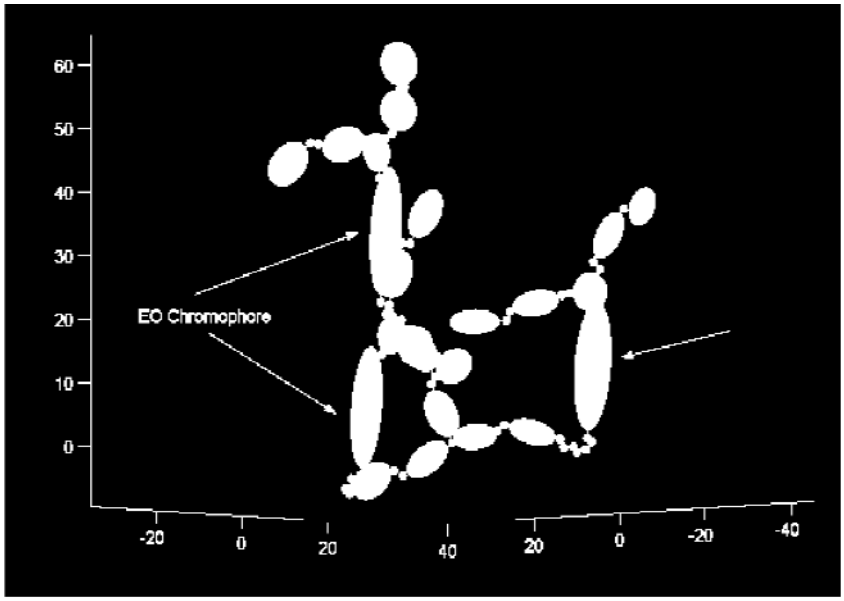

Fig. 4 Pseudo-atomistic Monte Carlo modeling of a three-chromophore dendrimer in a large poling field is shown. The chromophores are modeled as prolate ellipsoids. These are the larger ellipsoids shown in the figure. The smaller ellipsoids correspond to aromatic groups such as benzene rings. Individual carbon and oxygen atoms appear as small circles.

Our statistical mechanical calculations suggest that a variety of dendritic structures can lead to improved electro-optic activity. Representative structures are summarized in Fig. 5. As an example, we note that the dendronized polymer structure shown in Fig. 6 yields and electro-optic activity (at 1.3-μm wavelength and 20 % CLD chromophore [19] loading) of 111 pm/V compared to the best values of 58 pm/V obtained for the same chromophore in a composite material (30 wt% CLD in APC host).

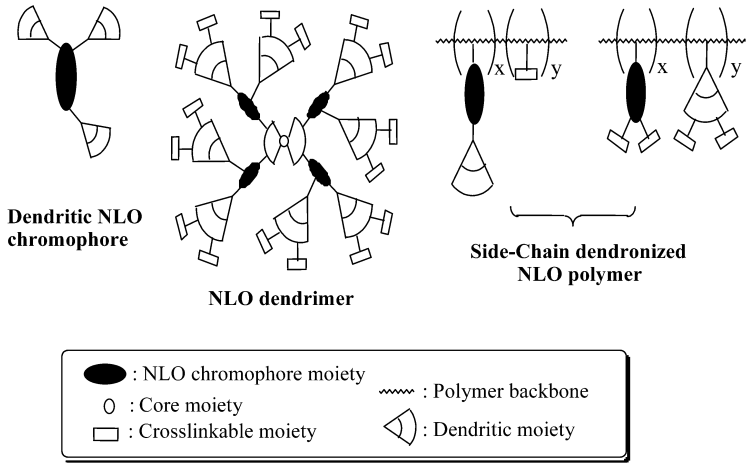

Fig. 5 Dendritic structures found to lead to improved electro-optic activity through improved $N\langle\cos^3\theta\rangle$ values are shown.

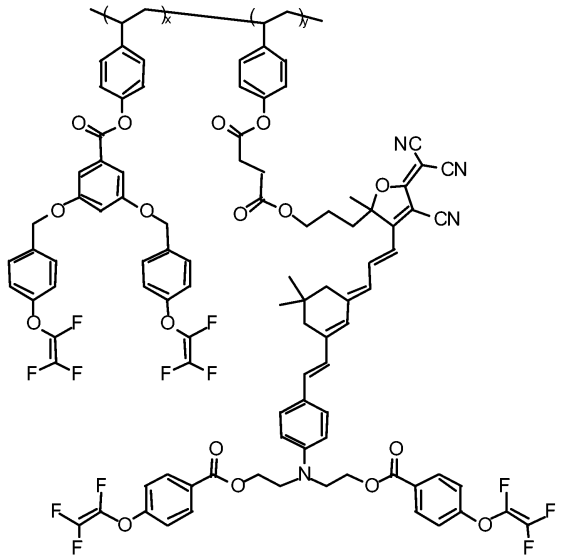

Fig. 6 The structure of a dendronized polymer leading to an electro-optic coefficient of 111 pm/V is shown. The chromophore is the CLD chromophore of ref. [21].

Recently, theory has suggested a variety of supramolecular architectures that may lead to improved noncentrosymmetric (ferroelectric) chromophore order under electric field poling. Several of these structures have been prepared and are now undergoing experimental evaluation in our laboratory. The prognosis is for significant improvements in electro-optic activity with preliminary observations of EO coefficients between 125 and 200 pm/V.

ORGANIC ELECTRO-OPTIC DEVICES

We have already noted that a variety of stripline, cascaded prism and superprism, and ring microresonator devices have been fabricated with organic electro-optic materials [7,13,42,43]. Moreover, conformal, flexible, and three-dimensional [25] active optical circuit structures and devices have been fabricated. Given the length limitations of this communication, we restrict our comments to flexible structures and recently prepared double-ring microresonator devices.

Conformal and flexible electro-optic devices

Analogous to organic light-emitting devices, organic electro-optic devices can be conformal and flexible in contrast to crystalline inorganic materials such as lithium niobate. This feature is important for applications such as phased array radar and particularly to space-based phased array radar antennae that are unfolded after delivery to orbit. To be usable for conformal and flexible device applications, properties such as drive voltage, optical loss, and bias voltage cannot change significantly with bending and flexing. We have observed this to be the case as is demonstrated by two representative examples (one involving optical loss characterization and one involving drive voltage characterization) shown in Figs. 7 and 8.

In Fig. 7, we show total optical insertion loss for a Mach Zehnder modulator, fabricated from organic electro-optic materials, as a function of bending about a cylinder of radius indicated in the figure. No significant change in optical loss is observed until bending radii of 1.5 mm are reached. Similar observations hold for other device properties for this test configuration. Our observations with respect to optical loss are consistent with our now extensive experience with ring microresonators where total op-

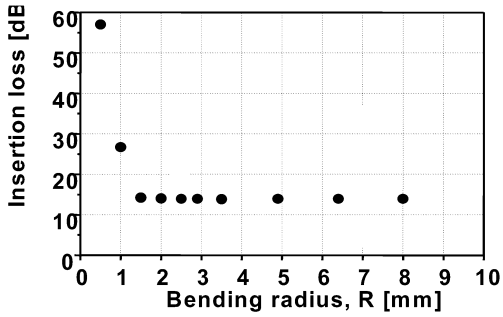

Fig. 7 Total insertion loss of an electro-optic device is shown as a function of bending about cylinders of radii indicated in the figure. The high value of insertion loss is due to "butt coupling" rather than use of a tapered transition to mode size match optical modes in the device and input and output waveguides. The precise value of total insertion loss is irrelevant for this test bed measurement; only changes with bending are of interest. Note that no change is observed until extreme bending radii of 1.5 mm are reached.

tical loss is defined by the combination of material, scattering, and bending loss [13,43]. Bending losses are, of course, determined by the radii of the ring microresonators and the index of refraction difference between the core and cladding materials (i.e., the greater the index difference, the smaller ring size that can be used).

In Fig. 8, we show a test bed for measuring the effect of flexing on device properties such as drive voltage (shown), optical loss, and bias voltage. As shown in Fig. 8, no significant change (within experimental error) in drive voltage (and other device properties not shown) is observed even with a high degree of flexing and repeated flexing.

We have previously demonstrated the unique advantages of organic electro-optic materials for fabricating three-dimensional circuit structures [13,15,25], which are particularly useful for compli-

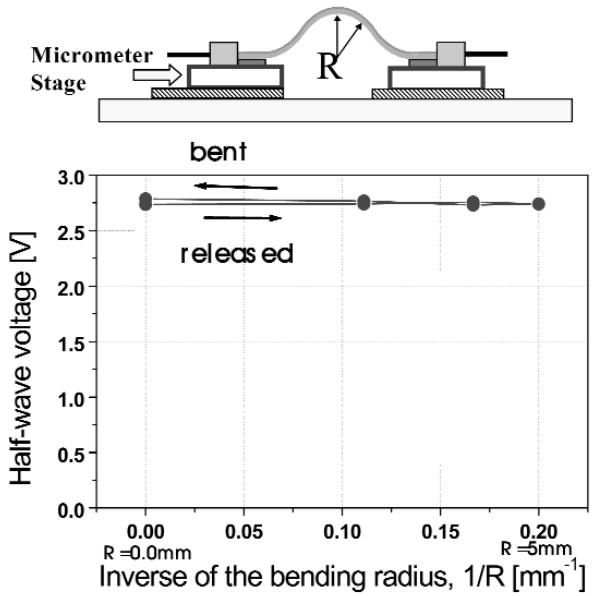

Fig. 8 Top: The test bed for measuring device properties with flexing is shown. Bottom: Typical performance of drive voltage with flexing is shown.

cated compact device structures for applications such as phased array radar and active wavelength division multiplexing. Here, the further advantage of permitting flexible and conformal devices to be fabricated is noted. In environments where device size is an issue or where mechanical vibration is a factor, the unique characteristics of organic electro-optic materials can be a compelling advantage.

Double-ring microresonators

Ring microresonators fabricated from organic electro-optic materials permit wavelengths to be selected with voltage control to a resolution of 0.01 nm (resulting from the fact that rings with quality factors, Q, of 10^5–10^6 are straightforwardly fabricated) [43]. Wavelength selectivity relates to two conditions must be satisfied for light to be coupled into a ring microresonator: (1) The circumference of the ring must be a multiple of the wavelength of the resonant light (the difference between two modes supported in such a resonator is called the free spectral range, FSR). (2) The velocity of light in the ring must match the velocity of input light (electro-optic tuning of the index of refraction of the ring permits this second condition to be satisfied with voltage control). Double-ring microresonators have the added condition provided by the Vernier effect that for light to go from the input to the drop port, both rings must be in resonance. Again, electro-optic tuning permits the two microresonator rings to be brought into resonance by voltage control.

The Vernier effect permits the rate of wavelength tuning of the drop port (output) mode to be amplified by shifting the matching of various resonance modes of the two ring resonators. In Fig. 9, we show the tuning of the output of an erbium optical amplifier over a 40-nm range by using a double-ring resonator with a tuning enhancement factor ($M = [1 - r_1/r_2]^{-1}$) of 40. The side mode suppression is greater than 30 dB. The FSR of this device (fabricated with rings of 480 and 492 μm) was 120 GHz.

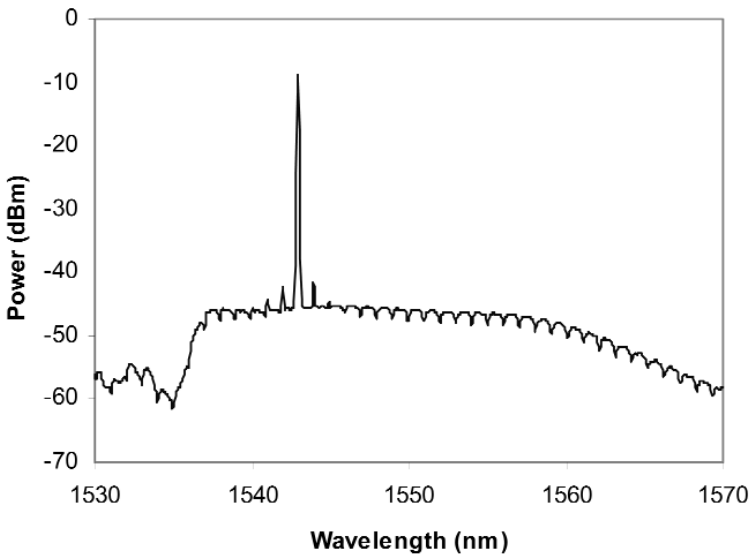

Fig. 9 Electro-optic tuning of the output of an erbium amplifier EDFA across the 1530–1570 nm spectral range is shown.

Recently, Prof. Amnon Yariv of California Institute of Technology has extended the concept double ring resonators to multi-ring resonators. A number of applications for such devices (e.g., active wavelength division multiplexing, optical reconfigurable interconnection, wavelength tuning of lasers, active wavelength filtering) can be anticipated.

ACKNOWLEDGMENTS

I gratefully acknowledge the contributions to this communication made by my graduate students and postdoctoral fellows and my many faculty colleagues, but most especially by Profs. William Steier, Alex Jen, and Bruce Robinson and their students and postdoctoral fellows. I also acknowledge the National Science Foundation (Grants DMR-0092380, 0103009, and 0120967) and the Air Force Office of Scientific Research for financial support of this research.

REFERENCES

1. J. L. Oudar. *J. Chem. Phys*. **67**, 446 (1977).
2. J. Zyss. *J. Mol. Elect*. **1**, 25 (1985).
3. L. A. Hornak. *Polymers for Lightwave and Integrated Optics*, Marcel Dekker, New York (1992).
4. G. A. Lindsay and K. D. Singer. *Polymers for Second-Order Nonlinear Optics*, American Chemical Society, Washington, DC (1995).
5. H. S. Nalwa and S. Miyata. *Nonlinear Optics of Organic Molecules and Polymers*, CRC Press, Boca Raton, FL (1997).
6. D. L. Wise, G. Wnek, D. J. Trantolo, T. M. Cooper, J. D. Gresser. *Electrical and Optical Polymer Systems*, Marcel Dekker, New York (1998).
7. L. R. Dalton. *Adv. Polym. Sci*. **158**, 1 (2002).
8. M. Lee, H. E. Katz, C. Erben, D. M. Gill, P. Gopalan, J. D. Heber, D. J. McGee. *Science* **298**, 1404 (2002).
9. D. Chen, D. Bhattacharya, A. Udupa, B. Tsap, H. R. Fetterman, A. Chen, S. S. Lee, J. Chen, W. H. Steier, L. R. Dalton. *IEEE Photon. Technol. Lett*. **11**, 54 (1999).
10. D. R. Kanis, M. A. Ratner, T. J. Marks. *Chem. Rev*. **94**, 195 (1994).
11. J. R. Heflin, K. Y. Wong, O. Zamani-Khamiri, A. F. Garito. *Phys. Rev. B* **38**, 1573 (1988).
12. S. R. Marder, C. B. Gorman, F. Meyers, J. W. Perry, G. Bourhill, J. L. Bredas, B. M. Pierce. *Science* **265**, 632 (1994).
13. L. R. Dalton. *J. Phys. Condens. Matter* **15**, R897 (2003).
14. L. R. Dalton, A. W. Harper, B. H. Robinson. *Proc. Natl. Acad. Sci. USA* **94**, 4842 (1997).
15. L. Dalton, A. Harper, A. Ren, F. Wang, G. Todorova, J. Chen, C. Zhang, M. Lee. *Ind. Eng. Chem. Res*. **38**, 8 (1999).
16. B. H. Robinson and L. R. Dalton. *J. Phys. Chem*. **104**, 4785 (2000).
17. L. R. Dalton, B. H. Robinson, R. Nielsen, A. K. Y. Jen, W. H. Steier. *Proc. SPIE* **4798**, 1 (2002).
18. L. R. Dalton, B. H. Robinson, A. K. Y. Jen, W. H. Steier, R. Nielsen. *Opt. Mater*. **21**, 19 (2003).
19. R. N. Nielsen, H. L. Rommel, B. H. Robinson. *J. Phys. Chem*. In press.
20. L. Dalton, A. Jen, W. Steier, B. Robinson, S. H. Jang, O. Clot, H. C. Song, Y. H. Kuo, C. Zhang, P. Raibiei, S. W. Ahn, M. C. Oh. *Proc. SPIE* **5351**, 1 (2004).
21. Y. Shi, C. Zhang, H. Zhang, J. H. Bechtel, L. R. Dalton, B. H. Robinson, W. H. Steier. *Science* **288**, 119 (2000).
22. Y. Shi, W. Lin, D. J. Olson, J. H. Bechtel, H. Zhang, W. H. Steier, C. Zhang, L. R. Dalton. *Appl. Phys. Lett*. **77**, 1 (2000).
23. W. K. Kim and L. M. Hayden. *J. Chem. Phys*. **111**, 5212 (1999).
24. S. S. H. Mao, Y. Ra, L. Guo, C. Zhang, L. R. Dalton, A. Chen, S. Garner, W. H. Steier. *Chem. Mater*. **10**, 146 (1998).
25. S. M. Garner, S. S. Lee, V. Chuyanov, A. Chen, A. Yacoubian, W. H. Steier, L. R. Dalton. *IEEE J. Quantum Electron*. **35**, 1146 (1999).
26. A. Chen, V. Chuyanov, F. I. Marti-Carrera, S. M. Garner, W. H. Steier, J. Chen, S. S. Sun, L. R. Dalton. *Opt. Eng*. **39**, 1507 (2000).
27. D. M. Burland, R. D. Miller, C. A. Walsh. *Chem. Rev*. **94**, 31 (1994).

28. L. R. Dalton, A. W. Harper, B. Wu, R. Ghosn, J. Laquindanum, Z. Liang, A. Hubbel, C. Xu. *Adv. Mater*. **7**, 519 (1995).
29. L. R. Dalton, A. W. Harper, R. Ghosn, W. H. Steier, M. Ziari, H. Fetterman, Y. Shi, R. Mustacich, A. K. Y. Jen, K. J. Shea. *Chem. Mater*. **7**, 1060 (1995).
30. J. Luo, S. Liu, M. Haller, H. Li, T. D. Kim, K. S. Kim, H. Z. Tang, S. H. Kang, S. H. Jang, H. Ma, L. R. Dalton, A. K. Y. Jen. *Proc. SPIE* **4991**, 520 (2003).
31. A. Galvan-Gonzalez, K. D. Belfield, G. I. Stegeman, M. Canva, S. R. Marder, K. Staub, G. Levina, R. J. Twieg. *J. Appl. Phys*. **94**, 756 (2003).
32. C. Zhang, L. R. Dalton, M.-C. Oh, H. Zhang, W. H. Steier. *Chem. Mater*. **13**, 3043 (2001).
33. P. A. Sullivan, S. Bhattacharjee, B. E. Eichinger, K. Firestone, B. H. Robinson, L. R. Dalton. *Proc. SPIE*, **5351**, 253 (2004); B. E. Eichinger, unpublished results.
34. S. P. Ermer, D. G. Girton, L. J. Dries, R. E. Taylor, W. D. Eades, T. E. Van Eck, A. S. Moss, W. W. Anderson. *Proc. SPIE* **3949**, 148 (2000).
35. M. He, T. M. Leslie, J. A. Sinicropi. *Chem. Mater*. **14**, 4662 (2002).
36. M. He, T. M. Leslie, J. A. Sinicropi, S. M. Garner, L. D. Reed. *Chem. Mater*. **14**, 4669 (2002).
37. S. Liu, M. A. Haller, H. Ma, L. R. Dalton, S. H. Jang, A. K. Y. Jen. *Adv. Mater*. **15**, 603 (2003).
38. C. Zhang, A. W. Harper, D. S. Spells, L. R. Dalton. *Synth. Commun*. **30**, 1359 (2000).
39. C. Zhang, A. W. Harper, L. R. Dalton. *Synth. Commun*. **31**, 1361 (2001).
40. J. Luo, S. Liu, M. Haller, H. Li, T. D. Kim, K. S. Kim, H. Z. Tang, S. H. Kang, S. H. Jang, H. Ma, L. R. Dalton, A. K. Y. Jen. *Proc. SPIE* **4991**, 520 (2003).
41. H. Ma, B. Chen, S. Takafumi, L. R. Dalton, A. K. Y. Jen. *J. Am. Chem. Soc*. **123**, 986 (2001).
42. L. Sun, J. Kim, C. Jang, D. An, X. Lu, Q. Zhou, J. M. Taboada, R. T. Chen, J. J. Maki, S. Tang, H. Zhang, W. H. Steier, C. Zhang, L. R. Dalton. *Opt. Eng*. **40**, 1217 (2001).
43. P. Rabiei, W. H. Steier, C. Zhang, L. R. Dalton, *J. Lightwave Technol*. **20**, 1968 (2002).